Impact of High Penetration of PV Generation on Frequency and Voltage in a Distribution Feeder

S.A. Pourmousavi, *Student Member*, *IEEE*, A.S. Cifala, and M.H. Nehrir, *Fellow*, *IEEE*

***Abstract*—This paper presents an evaluation of the impact of various levels of photovoltaic (PV) power penetration in a distribution feeder connected to a simplified grid model (SGM). PV generation is implemented in second-by-second iterations with power output based on actual solar radiation and air temperature data. High penetration levels of intermittent PV generation (15% and 30%) are employed in a feeder-configured microgrid to evaluate grid frequency and voltage characteristics. In this study, only governor droop control is included in the proposed SGM without the secondary control action (known as load frequency control). Two different grid models (fast and slow grid), PV generation configurations (concentrated and distributed), and PV penetration levels (15% and 30%) are considered in the simulation studies. Simulation results indicate the impact of the aforementioned parameters on the system frequency and voltage. Results also reveal that distributed PVs in a wide geographical area with different weather regime have less impact on the frequency and voltage.**

***Index Terms*— Distributed generation, frequency and voltage regulation, governor droop control, microgrid, PV penetration.**

I. Introduction

THE drive to provide more economical means of power production has resulted in major technological advances toward the application of distributed generation (DG). In turn, the practicality of alternative energy system deployment has become much more apparent. One such rapidly developing technology is solar photovoltaic (PV) power generation. The evolution of distributed PV is made evident by the 878 MW increase in grid-connected PV capacity in the US in 2010- nearly a 72% rise in capacity from 2009 [1]. However, the growing amount of penetration of DG (in particular intermittent renewable DGs, such as PV) can impact reliable operation of distribution system, to which they are connected [2].

The ability to balance generation and demand within a grid is imperative to maintaining electrical stability. At the distribution level, the impact of several highly variable sources such as PV can result in deviations in grid characteristics large enough to violate standard practices for implementation [3]. As the amount of grid-connected DG increases, grid operation and control becomes progressively more difficult and it may ultimately result in system failure. Consequently, dividing the main grid into smaller subsystems of microgrids presents a much more manageable and controllable network. This allows for higher penetration of reliable power sources, such as PV, without requiring massive architectural reconstruction of the main grid [4]. Additionally, microgrids provide greater system flexibility through the installation of inverter-interfaced inertia-less distributed generation systems (such as PV systems and fuel cells), as well as introducing adjustable base-load generators and energy storage systems to compensate for the variable generation that some renewable energy generation sources naturally exhibit [5], [6].

In this study, a grid-tied distribution feeder with concentrated or distributed PV resembles a microgrid. Since higher penetration of renewable resources into the conventional grid is desired, evaluation of their variable generation on the system's frequency and voltage is necessary. In order to avoid complex modeling of the grid, a simplified grid model (SGM) is developed at the distribution level to resemble the behavior of the actual grid at that level. Only governor droop control is considered for the grid in this study. No spinning reserve is included. The main purpose of this study is to investigate the actual impacts of large penetration of PVs in the order of seconds, whereas spinning reserves work in the order of minutes. The distribution feeder as a part of the grid is connected to the SGM to show the effects of variable PV generation on the system frequency and voltage. Two different SGMs (a slow and a fast response), and PV penetration values of 15% and 30% are studied. The PV generation is modeled as a PV farm and as distributed (customer owned) PV systems, as shown in Fig. 1 (a), (b).

Second-by-second solar insolation data is used to show the effects of abrupt variations in solar insolation. The SGM tries to adjust its output with variations in PV generation output to stabilize the system frequency and consequently voltage through its governor droop control. However, large penetration of PV generation causes the system frequency to fall out of the acceptable range most of the times. In a real system, load frequency control (LFC) could compensate for some of the above frequency deviations. The addition of these features as well as load control (Demand Response (DR)) for frequency stabilization is a part of our future work.

This work was in part supported by Pacific Northwest National Laboratory (PNNL), which is operated for the U.S. Department of Energy by Battelle under Contract DE-AC05-76RL01830, and by the DOE Award DE-FG02-11ER46817.

S.A. Pourmousavi (email: s.pourmousavikani@msu.montana.edu), Andrew S. Cifala (email: andrewcifala@gmail.com), and M.H. Nehrir (email: hnehrir@ece.montana.edu) are with the Electrical and Computer Engineering Department, Montana State University, Bozeman, 59717 USA.

Simulation results show the significant impact of high PV penetration on the system frequency and consequently voltage; however, the impact is lower in the case of distributed PVs compared to concentrated PVs (solar farm) with the same penetration level. It has also been shown that a larger grid with slow-response generators experience larger variations in system frequency and voltage. All system models are developed and tested in MATLAB/Simulink® [7].

The rest of the paper is organized as follows: Section II describes the system models and configurations developed for testing. Simulation results for each scenario are shown and discussed in Section III. The conclusions and plan for continuation of the current work are given in Section IV.

II. Systems Studied

The systems of study are modeled as grid-tied microgrids with concentrated or distributed PV DGs, as shown in Fig. 1 (a), (b). In both cases, the SGM with speed governor and exciter is utilized as presented in section II.A. The SGM is designed to resemble the actual behavior of a grid at the distribution level. It includes governor droop control, but LFC is not considered. The main objective of this study is to show the impact of medium and high levels of PV generation on the system frequency and voltage where only governor droop control is available for frequency regulation.

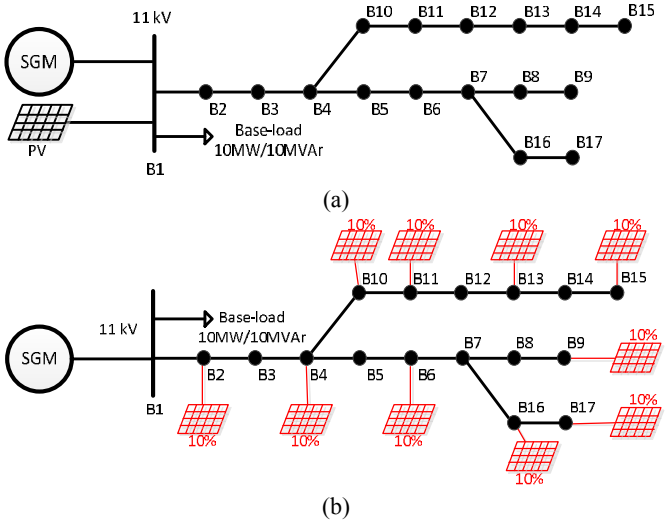

Fig. 1. Configuration of the generic feeder (a) with concentrated PV generation, and (b) distributed PV generation.

The PV model obtained from [8] is used. The model incorporates a maximum power point tracking (MPPT) system consisting of 30 kW PV arrays with a buck-boost DC/DC converter and a DC/AC inverter. The PV output power is scaled to achieve the desired level of penetration based on the number of arrays in the system. The inputs to the PV system are solar insolation and air temperature, which are recorded in one-second and one-minute intervals, respectively. The data is obtained from the National Renewable Energy Laboratory (NREL) for Oahu, Hawaii Solar Measurement Grid [9]. This solar insolation data is especially attractive for this study since the one-second data gives more accurate representation of the variable nature of PV output power during sporadic clouding, thus providing a more realistic case. To expose the variability issues with PV generation, solar irradiation is represented for a sunny day with erratic clouding (June 18, 2010).

Penetration by renewables can be defined in a number of ways (i.e., percentage of *energy* supplied by renewables, rated renewable power generation in comparison to peak load, and renewable generation in comparison to system capacity) [10]. In this study, PV penetration is defined as the rated PV capacity in relation to total capacity of the grid. 15% and 30% PV penetration level is studied.

A. Simplified Grid Model (SGM)

In the majority of power system studies, the grid is modeled as an infinite bus, which can provide or absorb any amount of power requested by loads. However, this is unacceptable in reality and also for the sake of this study, where system frequency and voltage are investigated under transient and steady-state conditions. Computationally, it is not always feasible to use a detailed grid model, such as this study. Thus, a simplified grid model is required at the distribution level, which can be utilized for any frequency and voltage stabilization studies, demand response studies and for evaluating the impact of renewable energy on the distribution grid. All the generators in the grid are modeled as a single generator with effective inertia of the grid, governor action, and load-frequency dependence [11], where the capacity of the grid model is the total capacity of the grid. The components of the proposed model are shown in Fig. 2.

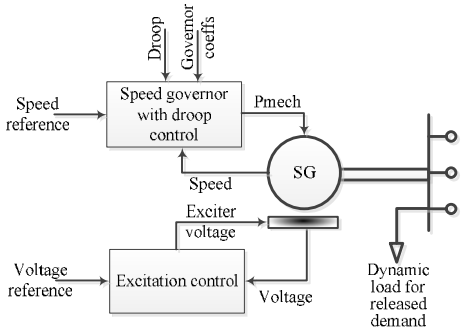

Fig. 2. Components of the proposed SGM.

The proposed model includes a synchronous generator, speed governor, voltage controller (excitation system), and a dynamic load. It is equipped with a type AC4A exciter with transient gain reduction [11], [12]. This model includes the following characteristics of an actual grid:

A. Governor droop characteristic can be applied to calculate the target mechanical power of the generator as follows [11], [13]:

$$P_{tar} = \left(\frac{f_{sp} - f_{act}}{R \times f_{nom}} \right) \ p.u. \qquad (1)$$

where f_{sp} is the frequency setpoint, f_{act} is the measured frequency, and f_{nom} is the nominal frequency, all in Hz. R is the droop value of the generator. Typically, speed governors are designed with 4%-20% "droop" characteristic [13]. For 4% droop value, the generator output will increase to 100% for a 4% drop in frequency.

B. The speed governor and turbine model. This model, shown in Fig. 3, is extracted from [12]. In Fig. 3, ω_{act} is the

measured machine radian speed, ω_{ref} is the machine reference speed, P_{tar} is the reference target power, and P_{mech} is the mechanical power driving the generator, all in per unit. Also, T_s is the servo time constant, T_C is the high pressure (HP) turbine time constant, T_3 is the transient gain time constant, T_4 is the time constant to set HP ratio, and T_5 is the re-heater time constant, all in sec [12].

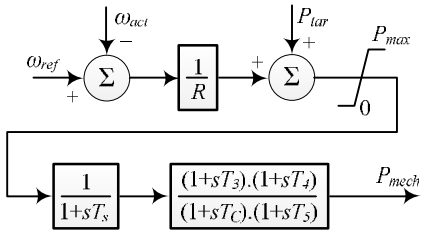

Fig. 3. Speed governor of the proposed SGM.

C. Released demand consisting of the loads which have built-in frequency dependence. When the frequency drops, the power consumption of such loads will drop as well and vice versa. This effect can be modeled by a variable active load model defined by Eq. (2) [11], [13]:

$$P_R = D.P_L.\left(\frac{f_{act} - f_{nom}}{f_{nom}}\right) ,W \qquad (2)$$

where D is the load-damping constant, and P_L is the total amount of active load, including the released demand.

D. Inertia of an actual power system which typically varies between 2 and 8 sec [11], [13]. This effective inertia is used in the inertia of single synchronous generator.

E. Total generation capacity of the grid can also be modeled as the capacity of a single large synchronous generator. The impedance of the single generator is tuned to result in the typical losses of the desired power system.

B. Feeder Configured Microgrid

The system incorporates distributed aggregated loads in a grid-tied microgrid configured as a generic feeder, as shown in Fig. 1 (a), (b). The parameters of the lines and aggregated loads are obtained from a study on distribution system reconfiguration [14]. However, the grid in [14] is replaced by the proposed SGM in this paper. In Fig. 1 (a), the PV DG is implemented as a single concentrated source. This scenario represents a solar PV farm where all PV panels experience the same weather regime. The farm is sized to the desired level of penetration. The total load of the feeder is approximately 0.837 MW/0.626 MVAr for a total of approximately 1.06 MVA. The total resistive and reactive load for the top, middle, and bottom branches of the feeder are 0.256 MW/0.189 MVAr, 0.447 MW/0.352 MVAr, and 0.140 MW/0.085 MVAr, respectively. This feeder is considered as the added load to a grid with 10 MW/10 MVAr base-load. The released demand is implemented for the active base-load in the SGM. Simulations are performed with the concentrated PV system scaled to penetration levels of 15% and 30%, corresponding to 4.5 MW (150 30-kW arrays) and 9.0 MW (300 30-kW arrays), respectively.

To investigate the effect of the distributed PVs, an additional scenario is tested, where the PV arrays are distributed at arbitrary nodes within the feeder, as shown in Fig. 1 (b). This scenario is intended to represent distributed PV throughout a community of loads. The total PV penetration capacity is distributed at 10 different nodes in the feeder, assumed to be in a large geographical area. It is also assumed that each PV station at each node is the aggregate of several distributed PV units in a geographical area with similar solar insolation and temperature regime. The total PV penetration capacity is the same as in the concentrated PV case. To emulate the moving clouds, insolation for each PV system is lagged for an arbitrarily chosen time of 500 seconds (just over eight minutes). This delay represents a moving cloud in the area with several small PV generation units.

In power systems, a negative frequency deviation is an indication of excess load or lack of generation, while positive frequency deviation suggests a lack of demand or excess generation [12], [13], [15]. It is well known that mitigating the large deviations in frequency is crucial for restoring system stability; therefore, loads must be released or added according to the situational frequency in emergency circumstances. In North America, whenever a frequency error persists for a certain time (10 seconds for the east, 3 seconds for Texas, and 2 seconds for the west), a correction of ±0.02 Hz (0.033% of 60 Hz) is applied [15]. This corrective action starts with primary frequency regulation, and follows by secondary and tertiary frequency regulation, just in case. Since spinning reserves are expensive, and their use result in higher marginal cost of electricity, it is always desired to avoid purchasing spinning reserve for frequency regulation. Therefore, this study is undertaken to show the impact of high levels of PV generation with only governor droop control which finally translates to a need for a required amount of spinning reserve. In other words, larger frequency variations require more spinning reserve. As another possibility for providing ancillary services in place of spinning reserve, DR is known as a promising technology in smart grid for frequency regulation [16], [17]. LFC could help partially reduce the frequency variations; however, because its response is not as fast as governor droop control, it is unlikely that the combination of governor droop control and LFC could reduce all the frequency variations [18]. We therefore plan to investigate both the effect of LFC as well as DR for frequency regulation in our future work.

III. Simulation Results

The systems described are simulated in MATLAB/Simulink® to evaluate their operational characteristics. The system is evaluated over a 9000-second (hrs: 12:36-15:06) portion of the day for the solar insolation and temperature curves shown in Fig. 4 (a), (b). This time-span is chosen because of large fluctuations in insolation and therefore PV output power. The insolation data reaches near 1000 W/m^2 (standard maximum insolation) at its peak value. This helps maintain consistency in the rated peak power output of the PV system and, ultimately, accuracy when defining the level of penetration.

Multiple case studies are developed, including variations in the SGM characteristics, PV penetration level and configuration. The grid operation is evaluated through the different characteristics of the grid at the point of connection.

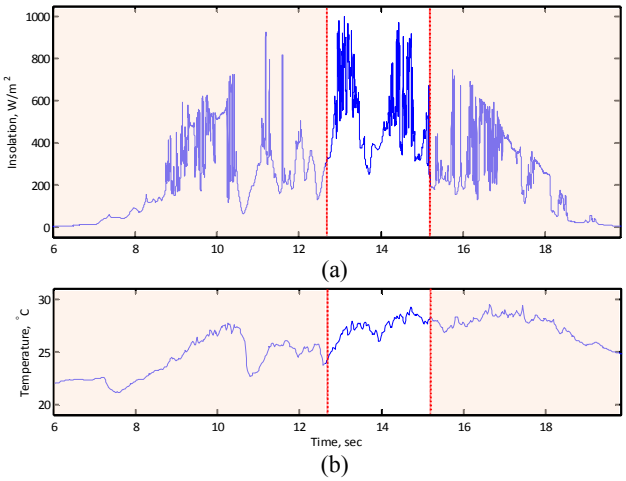

Fig. 4. (a) Solar insolation and (b) air temperature.

Two different grid characteristics are examined in this study. The first grid model (SGM1) approximates a grid with slow response generators, such as the Western North American power grid with many hydro generators. The governor droop for all of the generators in this power system is set to 20% [12]. The second one (SGM2) resembles a fast response grid with small-sized turbo or diesel generators, such as Lanai in Hawaii [19]. It consists of two isochronous 2.8 MVA diesel generators and two frequency-droop 1.2 MVA diesel generators with 4% droop [19]. The specifications of these two grids in SGM are shown in Table I.

TABLE I
THE SGMS PARAMETERS

	SGM1 (slow)	SGM2 (fast)
Synchronous Generator Parameters		
x_d (pu)	0.9	1.9
x'_d (pu)	0.27	0.27
T'_{d0} (sec)	9.0	6.0
x_q (pu)	0.6	1.6
x'_q (pu)	0.27	0.27
T'_{q0} (sec)	0.05	0.8
H (sec)	4.4	4.0
Governor Parameters		
Droop (pu)	0.2	0.04
P_{max} (pu)	1.0	1.0
T_s (sec)	0.4	0.04
T_c (sec)	75.0	0.2
T_3 (sec)	10.0	0.0
T_4 (sec)	2.4	1.5
T_5 (sec)	1.2	5.0
Exciter Parameters		
K_A	150	200
T_A (sec)	0.09	0.04
V_{max}, V_{min} (pu)	6.0/-3.0	6.0/-3.0

For ease of comparison, the total capacity of the system for both SGMs is chosen to be 30 MVA. The base-load of the system is considered to be 10 MW/10MVAr, and the feeder load of 0.837 MW/0.626 MVAr is added to the base-load.

A. 15% PV penetration

In this case, the impact of 15% PV generation is evaluated on the performance of the system for the two grid models. Results for the concentrated and distributed PV generation are given. To evaluate the voltage at different nodes within the feeder, measurements are taken at nodes at the end of the feeders, nodes B9, B15, and B17 in Fig. 1 (a), (b).

Case I: 15% Concentrated PV Generation

This case shows the effect of concentrated PV generation on the feeder with aggregated loads. As seen in Fig. 5 (a), the frequency is mostly outside the acceptable range (60±0.05 Hz), especially during the high PV generation hours. As it can be seen in Fig. 5 (a), the frequency fluctuations are less in the case of SGM2 compared with those in the case of SGM1. This indicates that the performance of grid at the point of connection is an important factor for increasing the penetration level of PV generation. In other words, a slow-response power system has a major barrier for increased PV penetration level. For ease of comparison, Table II shows the frequency statistics for both the grid models.

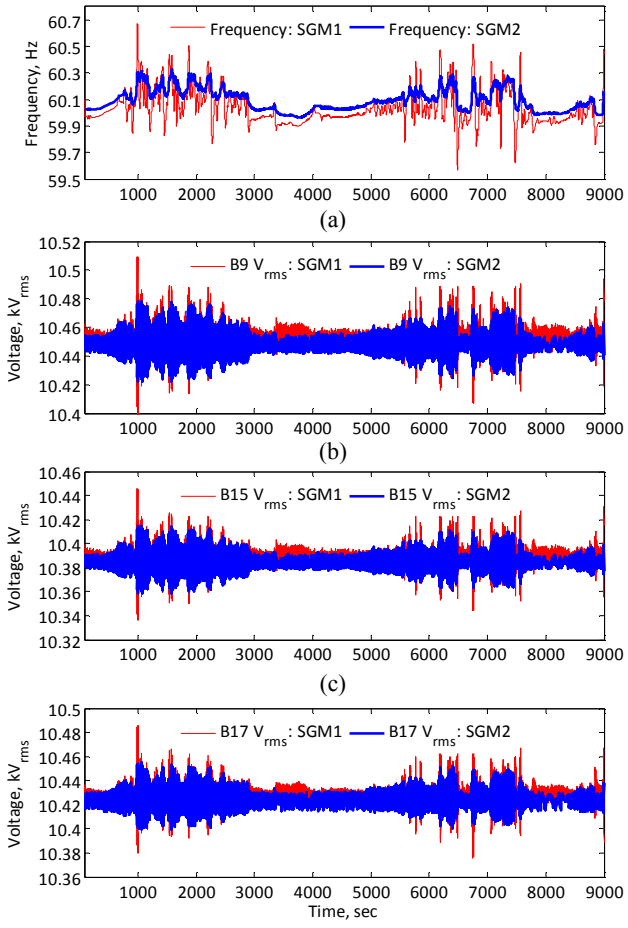

Fig. 5. (a) System frequency and voltages of nodes (b) B9, (c) B15, and (d) B17 for both models of the grid.

The root mean square error (RMSE), given in the table, is calculated as follows:

$$RMSE = \sqrt{\sum_{i=1}^{n} \left(f_{act} - f_{nom} \right)^2 \Big/ n} \qquad (3)$$

where n is the number of samples from simulations. It can be seen that the largest variations in the maximum and minimum frequency, standard deviation, and RMSE happen in the case of SGM1.

The voltage profiles at the feeder branches B9, B15, and B17 are shown in Fig. 5 (b)-(d), respectively. In this case, the deviations in voltage are minimal and have no negative impact on the system performance. However, voltage variations are slightly more in the case of SGM1 compared to SGM2.

TABLE II
SYSTEM FREQUENCY STATISTICS FOR BOTH SGMS IN CASE I

	Minimum frequency (Hz)	Maximum frequency (Hz)	Average frequency (Hz)	Standard deviation (Hz)	RMSE (Hz)
SGM1	59.57	60.67	60.03	0.128	0.133
SGM2	59.97	60.33	60.09	0.084	0.126

The mechanical output power for both the grid models and the total PV generation are shown in Fig. 6 (a). It can be seen that the variations in PV generation and mechanical output power from the SGMs are reversed. Although it seems that the output mechanical power for both SGMs is the same in Fig. 6 (a), they show different transient behaviors with very similar performance, as shown in Fig. 6 (b) (which shows the simulation results for 200 seconds). The similar performance is because the total generation and demand are almost the same in both cases. Since frequency is different in the two SGMs, the amount of frequency dependent load would be different, which finally causes slight difference in the output mechanical power of the two SGMs.

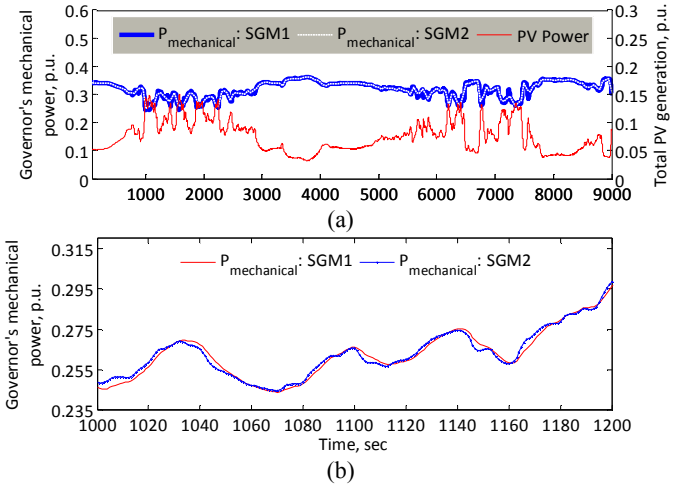

Fig. 6. (a) SGMs output mechanical power for 15% concentrated PV generation and total PV generation, and (b) zoomed-in output mechanical power of the SGMs.

Case II: 15% Distributed PV Generation

This case shows the effect of distributed PV generation on the feeder with aggregated loads. As seen in Fig. 7(a), the frequency is still out of the acceptable range; although the variations are much less compared to those of the concentrated PV generation. It basically shows that a higher level of penetration of PV generation is achievable if the generation is distributed in a large area with different weather regime. These variations are less in the case of SGM2 compared to those in SGM1 as a result of quick response of the speed governor in SGM2. Table III shows the frequency statistics for both the grid models. It can be seen that larger variations in frequency as well as standard deviation and RMSE happen in the case of the feeder with SGM1.

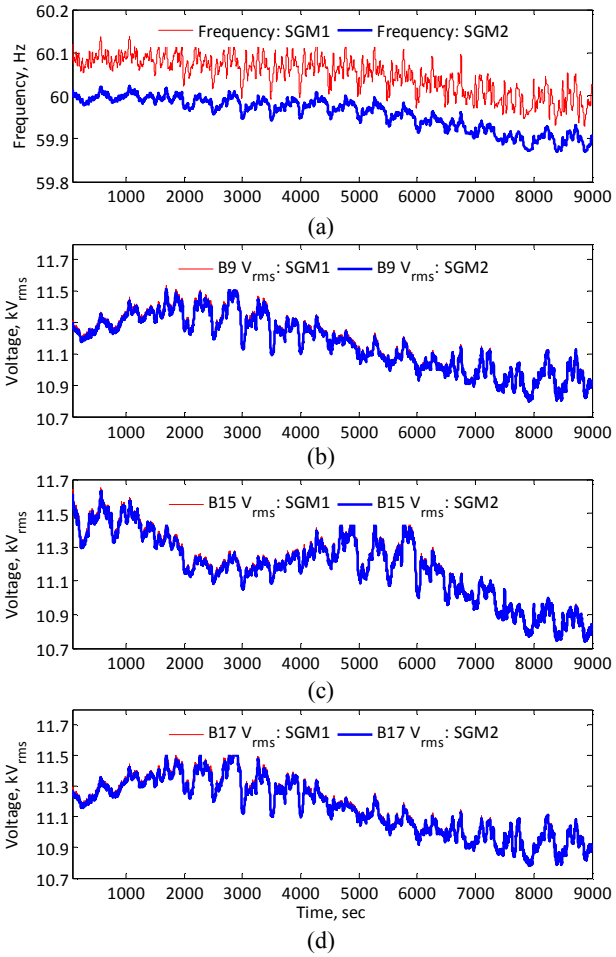

Fig. 7. (a) System frequency and voltages of nodes (b) B9, (c) B15, and (d) B17 for both models of the grid.

The voltage profiles at nodes B9, B15, and B17 are shown in Fig. 7 (b)-(d), respectively. Although the system frequency for distributed PV is reduced significantly compared to the concentrated PV generation case, the voltage deviations at the different nodes are considerably higher since the PV generation is distributed and is close to the load centers (consumers). As a result, the system power loss and distribution line loading are lower, and the node voltages (and also the voltage variations) are increased. This problem can be solved by installing smaller PV generation units at more distributed configuration. It can also be observed that there are no significant differences in the node voltages under the two SGMs.

TABLE III
SYSTEM FREQUENCY STATISTICS FOR BOTH SGMS IN CASE II

	Minimum frequency (Hz)	Maximum frequency (Hz)	Average frequency (Hz)	Standard deviation (Hz)	RMSE (Hz)
SGM1	59.93	60.14	60.05	0.043	0.064
SGM2	59.87	60.02	59.96	0.038	0.057

The output mechanical power for both the grid models and the total PV generation are shown in Fig. 8 (a). Again, it can be observed that the variations in the output mechanical power of SGMs are in such a way to compensate for the deficiency and excess of the PV generation. Fig. 8 (b) shows the zoomed-in output mechanical power of both SGMs, which are almost the same. However, SGM1 has slower response due to its slower governor action.

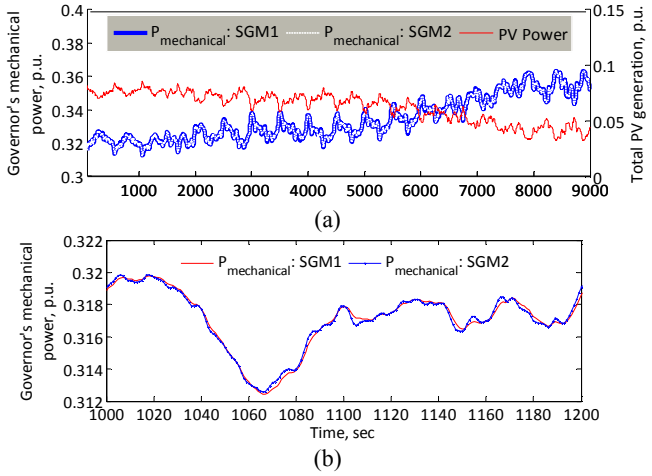

Fig. 8. (a) SGMs output mechanical power for 15% distributed PV generation and total PV generation, and (b) zoomed-in output mechanical power of the SGMs.

B. *30% PV penetration*

In this case, the impact of 30% PV penetration on the performance of the system for the two grid models is evaluated. The system frequency and node voltage variations for the concentrated and distributed PV generation are reported in the following two sub-sections.

Case III: 30% Concentrated PV Generation

This case shows the impact of 30% penetration of concentrated PV generation (as in Fig. 1 (a)) on the feeder with aggregated loads. As seen in Fig. 9 (a), the frequency varies significantly and is mostly outside the acceptable limits, 60±0.05 Hz. Particularly, the 30% penetration of PV generation has corruptive effects for the slower response grid, SGM1. These variations are more than five times greater than they were in the previous study, with 15% PV penetration. Table IV shows the frequency statistics for both SGMs. It can be seen that the system with SGM1 has a higher maximum frequency, lower minimum frequency, and higher standard deviation and RMSE.

The voltage profiles at nodes B9, B15, and B17 are shown in Fig. 9 (b)-(d), respectively. These figures show unacceptable variations in the node voltages, which are the result of large frequency deviation, in particular when SGM1 is used.

TABLE IV
SYSTEM FREQUENCY STATISTICS FOR BOTH SGMS IN CASE III

	Minimum frequency (Hz)	Maximum frequency (Hz)	Average frequency (Hz)	Standard deviation (Hz)	RMSE (Hz)
SGM1	59.14	67.32	60.32	0.636	0.711
SGM2	60.06	60.79	60.32	0.167	0.361

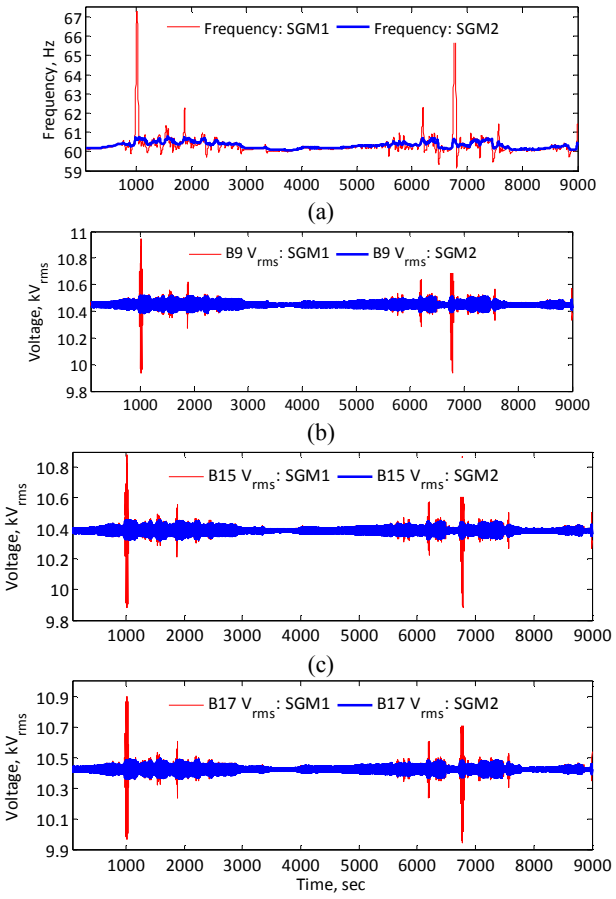

Fig. 9. (a) System frequency and voltages of nodes (b) B9, (c) B15, and (d) B17 for both models of the grid.

The output mechanical power for both SGMs and the total PV generation are shown in Fig. 10 (a). Similar pattern as in the case of 15% PV penetration exists for the output mechanical power in relation to the total PV generation can be observed, i.e. when PV generation is high, the output mechanical power of the SGMs are low and vice versa. Fig. 10 (b) shows a part of the output mechanical power for better observation of the variations. The effect of large variations in the frequency on the frequency dependent loads is clear in the case of SGM1, as shown in the first 50 seconds in Fig. 10 (b).

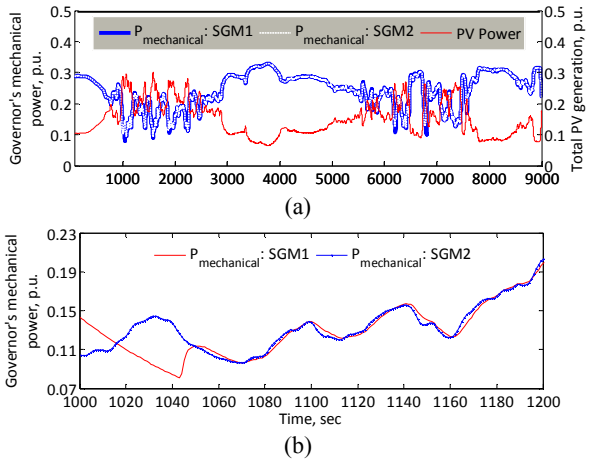

Fig. 10. (a) SGMs output mechanical power for 30% concentrated PV generation and total PV generation, and (b) zoomed-in output mechanical power of the SGMs.

It can be seen that the output mechanical power for the two SGMs are very close; however, they are different at the points when the frequency and voltage deviations in two SGMs are very different. As a consequence, these variations in mechanical power will result in load variations for both the frequency dependent and constant impedance loads.

Case IV: 30% Distributed PV Generation

This case shows the effect of 30% distributed PV generation on the feeder with aggregated loads. As seen in Fig. 11 (a), the frequency variations are still out of the acceptable range; however, these variations are less than those with 30% concentrated PV for both SGMs, Fig. 9 (a).

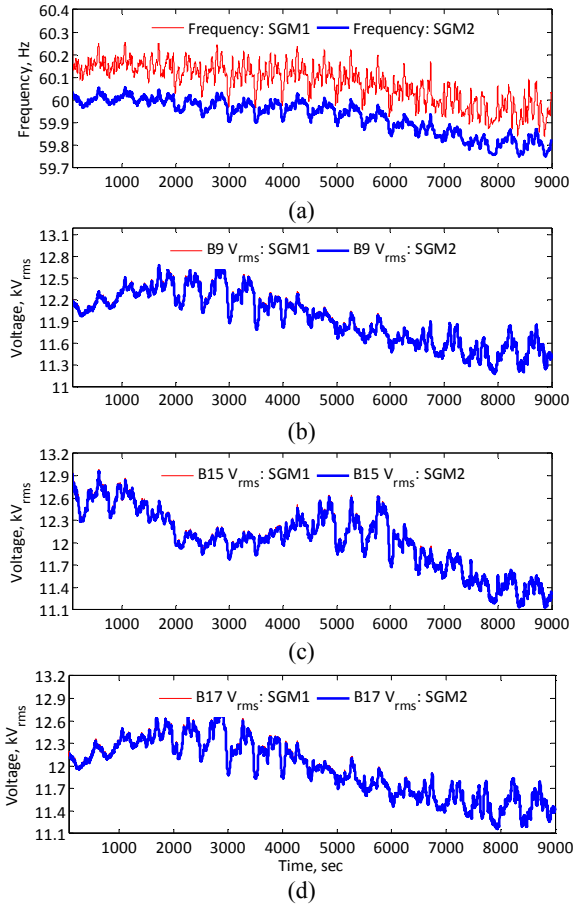

Fig. 11. (a) System frequency and voltages of nodes (b) B9, (c) B15, and (d) B17 for both models of the grid.

The variations are smaller in the case of SGM2 due to its quicker response. Therefore, it can be concluded that proper distribution of PV generation in a wide geographical area could have a better effect on the existing system than concentrated PV generation (i.e., a PV solar farm). Table V shows the frequency statistics for both SGMs for the 30% distributed PV generation. It can be seen that larger maximum frequency, and larger standard deviation and RSME occur with the slow SGM (SGM1).

The voltage profiles at nodes B9, B15, and B17 are shown in Fig. 11 (b)-(d), respectively. Voltage deviations are beyond the acceptable range, which is primarily a result of large PV generation installed very close to the consumer loads. There is no significant difference between voltages at the two SGMs.

TABLE V
SYSTEM FREQUENCY STATISTICS FOR BOTH SGMS IN CASE IV

	Minimum frequency (Hz)	Maximum frequency (Hz)	Average frequency (Hz)	Standard deviation (Hz)	RMSE (Hz)
SGM1	59.84	60.26	60.08	0.086	0.116
SGM2	59.75	60.06	59.93	0.076	0.105

The output mechanical power for both grid models and total distributed PV generation are shown in Fig. 12 (a). Also, the zoomed-in mechanical power is depicted in Fig. 12 (b) to show the difference in the transient response of the two SGMs. The response is always faster in the case of SGM2 compared to the one in SGM1 as a result of faster governor action.

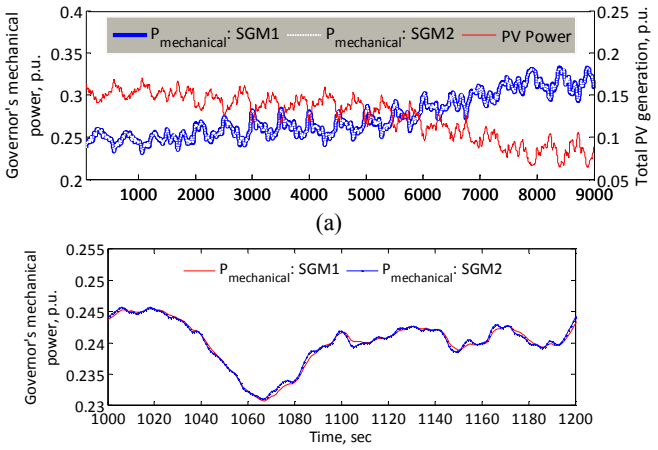

Fig. 12. (a) SGMs output mechanical power for 30% distributed PV generation and total PV generation, and (b) zoomed-in output mechanical power of the SGMs.

IV. CONCLUSIONS AND FUTURE WORK

This paper presents the effect of high penetrations of solar PV generation on frequency and voltage in a distribution feeder configured as a grid-tied microgrid. Different PV penetration levels, grid characteristics at the point of connection, and PV configuration in the microgrid are considered in the study. A simplified grid model is presented to resemble the grid at the distribution level. Only governor droop control is considered in the SGM. Simulation results indicate that a higher level of PV penetration is achievable through small-sized distributed PV generation or a grid with faster response. A distributed PV in a large area with different weather regimes could also be beneficial to achieve higher levels of PV penetration.

It is shown in this paper that the corrective action of the governor droop control of the SGMs is very limited in stabilizing the frequency and voltage in the distribution feeder. It is planned to continue the current work and include conventional ancillary services as well as customer participation through an effective demand response program for the stabilization of frequency and voltage under high penetration of solar PV generation.

REFERENCES

[1] Solar Energy Industries Association, *U.S. Solar Market Insight(TM): 2010 Year in Review* (Executive Summary), 2010, Solar Energy Industries Association.

[2] Thomas S. Basso, "High-Penetration, Grid-Connected Photovoltaic Technology Codes and Standards," *33rd IEEE Photovoltaic Specialists Conference*, pp. 1-6, 2008.

[3] IEEE STD 1547, *Standard for Interconnecting Distributed Resources with Electric Power Systems*, June 2003.

[4] P. Piagi, R. H. Lasseter, "Autonomous control of microgrids," *Proceedings,* IEEE PES General Meeting, Jun. 18–22, 2006.

[5] EU Project "MICROGRIDS: Large Scale Integration of Micro-Generation to Low Voltage Grids (ENK5-CT-2002-00610)," Website: http://microgrids.power.ece.ntua.gr/.

[6] P. Denholm, M. Hand, "Grid flexibility and storage required to achieve very high penetration of variable renewable electricity," Energy Policy, 2011.

[7] MATLAB/Simulink SimPowerSystems Documentation, Website: http://mathworks.com/.

[8] C. Wang, "Modeling and Control of Hybrid Wind/Photovoltaic/Fuel Cell Distributed Generation Systems," Ph.D. Dissertation, Montana State University, Bozeman, 2006.

[9] National Renewable Energy Laboratory (NREL), "NREL: MIDC/Oahu Irradiance Grid," Website: http://www.nrel.gov/midc/oahu_archive/.

[10] California Energy Commission's Intermittency Analysis Project Study, "Appendix B - Impact of Intermittent Generation on Operation of California Power Grid," Website: http://www.energy.ca.gov/2007publications/CEC-500-2007- 081/CEC-500-2007-081-APB.PDF.

[11] P. Kundur, Power System Stability and Control, McGraw-Hill Inc., 1994, ch. 11.

[12] D. Trudnowski, M. Donnelly, E. Lightner, "Power-System Frequency and Stability Control using Decentralized Intelligent Loads," In *Proc.,* IEEE PES Conference and Exhibition Transmission and Distribution, 2005, pp. 1453–1459.

[13] J.A. Short, D.G. Infield, L.L. Freris, "Stabilization of Grid Frequency Through Dynamic Demand Control," *IEEE Trans. on Power Syst.*, vol. 22, no. 3, 2007, pp. 1284–1293.

[14] D. Das, "A fuzzy multiobjective approach for network reconfiguration of distribution systems," *IEEE Trans. Power Del.*, vol. 21, no. 1, pp. 202–209, Jan. 2006.

[15] Y. G. Rebours, D. S. Kirschen, M. Trotignon, S. Rossignol, "A Survey of Frequency and Voltage Control Ancillary Services—Part I: Technical Features" , *IEEE Trans. on Power Systems*, vol. 22, no. 1, pp. 350–357, Feb, 2007.

[16] S.A. Pourmousavi, M.H. Nehrir, "Demand Response for Smart Microgrid: Initial Results," In *Proc.* 2nd IEEE PES Innovative Smart Grid Technologies (ISGT), 2011, pp. 1–6.

[17] S.A. Pourmousavi, M.H. Nehrir, C. Sastry, "Providing Ancillary Services through Demand Response with Minimum Load Manipulation," In *Proc.* North American Power Symposium (NAPS), 2011, pp. 1–6.

[18] J. D. Glover, M. S. Sarma, T. J. Overbye, *Power System Analysis and Design,* Stamford, CT, Cengage Learning, 2008, ch. 11.

[19] B. L. Schenkman, D. G. Wilson, R. D. Robinett III, "Photovoltaic Distributed Generation for Lanai Power Grid Real-Time Simulation and Control Integration Scenario," In *Proc.*, International Symposium on Power Electronics, Electrical Drives, Automation and Motion, 2010, pp. 154-157.

BIOGRAPHIES

S. Ali Pourmousavi (S'07) received the B.S. degree with honors from University of Mazandaran, Iran in 2005 and M.S. degree with honors from Amirkabir University of Technology (Tehran Polytechnic), Iran in 2008, all in electrical engineering. He is a Ph.D. student in the Electrical and Computer Engineering (ECE) Department at Montana State University, Bozeman, MT. His research interests include energy management of hybrid power generation systems, load control and demand response, and wind speed and power forecasting.

Andrew Stone Cifala (S'09) received the B.A. degree from Carroll College, Helena, Montana in 2009 in mathematics, an M.S. degree in the Electrical and Computer Engineering Department at Montana State University in 2011. His research interests include developmental innovative alternative energy, load control and demand response, and smart grid/microgrid integration.

M. Hashem Nehrir (S'68–M'71–SM'89–F'10) received the B.S., M.S., and Ph.D. degrees from Oregon State University, Corvallis, in 1969, 1971, and 1978, respectively, all in electrical engineering. He was with the Electrical Engineering Department, Shiraz University, Iran from 1971 to 1986. Since 1987, he has been on the faculty of the Electrical and Computer Engineering Department, Montana State University, Bozeman, MT, where he is a Professor. His research interests include modeling and control of power systems, alternative energy power generation systems, and application of intelligent controls to power systems. He is the author of three textbooks and an author or coauthor of numerous technical papers.